2014

Multi-agent receding horizon control with neighbour-to-neighbour communication for prevention of voltage collapse in a multi-area power system

Sk. Razibul Islam
University of Wollongong, sri703@uowmail.edu.au

Kashem M. Muttaqi
University of Wollongong, kashem@uow.edu.au

Danny Sutanto
University of Wollongong, soetanto@uow.edu.au

Publication Details

S. Islam, K. M. Muttaqi & D. Sutanto, "Multi-agent receding horizon control with neighbour-to-neighbour communication for prevention of voltage collapse in a multi-area power system," IET Generation, Transmission and Distribution, vol. 8, (9) pp. 1604-1615, 2014.

Multi-agent receding horizon control with neighbour-to-neighbour communication for prevention of voltage collapse in a multi-area power system

Abstract

In this study, a multi-agent receding horizon control is proposed for emergency control of long-term voltage instability in a multi-area power system. The proposed approach is based on a distributed control of intelligent agents in a multi-agent environment where each agent preserves its local information and communicates with its neighbours to find an optimal solution. In this study, optimality condition decomposition is used to decompose the overall problem into several subproblems, each to be solved by an individual agent. The main advantage of the proposed approach is that the agents can find an optimal solution without the interaction of any central controller and by communicating with only its immediate neighbours through neighbour-to-neighbour communication. The proposed control approach is tested using the Nordic-32 test system and simulation results show its effectiveness, particularly in terms of its ability to provide solution in distributed control environment and reduce the control complexity of the problem that may be experienced in a centralised environment. The proposed approach has been compared with the traditional Lagrangian decomposition method and is found to be better in terms of fast convergence and real-time application.

Disciplines

Engineering | Science and Technology Studies

Publication Details

S. Islam, K. M. Muttaqi & D. Sutanto, "Multi-agent receding horizon control with neighbour-to-neighbour communication for prevention of voltage collapse in a multi-area power system," IET Generation, Transmission and Distribution, vol. 8, (9) pp. 1604-1615, 2014.

Multi-agent Receding Horizon Control with Neighbour to Neighbour Communication for Prevention of Voltage Collapse in a Multi-area Power System

Sk Razibul Islam, Kashem M Muttaqi and Danny Sutanto
Endeavour Energy Power Quality and Reliability Centre
School of Electrical, Computer and Telecommunications Engineering
University of Wollongong, NSW 2522, Australia

Abstract:

In this paper, a multi-agent receding horizon control is proposed for emergency control of long-term voltage instability in a multi-area power system. The proposed approach is based on a distributed control of intelligent agents in a multi-agent environment where each agent preserves its local information and communicates with its neighbours to find an optimal solution. In this paper, optimality condition decomposition (OCD) is used to decompose the overall problem into several sub-problems, each to be solved by an individual agent. The main advantage of the proposed approach is that the agents can find an optimal solution without the interaction of any central controller and by communicating with only its immediate neighbours through neighbour-to-neighbour communication. The proposed control approach is tested using the Nordic-32 test system and simulation results show its effectiveness, particularly in terms of its ability to provide solution in distributed control environment and reduce the control complexity of the problem that may be experienced in a centralized environment. The proposed approach has been compared with the traditional Lagrangian decomposition method and is found to be better in terms of fast convergence and real-time application.

1.0 Introduction

Emergency voltage control has become an important task to be implemented by the power system control centre and has gained much attention among the research community, especially after several wide-spread black out events throughout the world in the last few decades [1, 2]. An added concern is the complicated situation to fulfil this task by the transmission system operator (TSO) arising from the large scale inter-connection of electric power system. Furthermore, reported incidents on voltage collapse has shown that the time-span between an initiating disturbance and system breakdown is too limited and too complex for the TSO to take manual control action to prevent the system from undergoing voltage instability [3]. According to the stability definition of IEEE/CIGRE task force [3], voltage stability refers to the ability of a power system to maintain steady voltages at all buses in the system after being subjected to a disturbance from a given initial operating condition. Instability that may result occurs in the form of a progressive fall or rise of voltages of some buses. Voltage collapse refers to the process by which the sequence of events accompanying voltage instability leads to a blackout or abnormally low voltages in a significant part of the power system. As a result, many automatic voltage control schemes have been proposed in the literature that deal with the real time assessment of the control system to avoid voltage collapse during emergency condition involving several coincident disturbances [4] [5] [6].

Recently, many emergency voltage control strategies have been developed using the concept of Receding Horizon Control (RHC) (also known as Model Predictive Control (MPC)) [7 - 15]. RHC is a special class of online control strategies in which the control actions and closed-loop feedback of the system are computed at each moving window of time rather than at a single time instance. In the context of voltage control, this strategy helps to take advantage of the dynamic system evolution and to provide a feasible transition to stable system equilibrium. A pioneering work using RHC technique is the co-ordinated secondary voltage control addressed in [6]. In this study, the original predictive control scheme is separated into two sub-problems, namely the *static* and *dynamic* sub-problems taking into account the transmission delays and asynchronous measurement. A tree search method has been employed in [8] to co-ordinate the generator voltages, tap-changers and load shedding in the RHC approach and an Euler State predictor (ESP) has been used to predict the output state trajectories. Reference [9] also used ESP based on non-linear system equations and the optimization problem was solved using pseudo-gradient evolutionary programming (PGEP). A RHC based real time system protection scheme against voltage instability by means of capacitor switching is proposed in [10]. A receding horizon multi step optimization has been used in [11] based on the steady state power-flow equations to alleviate unacceptable voltage profile. The evolution of the load power restoration due to On Load Tap Changing Transformers (OLTCs) and the activation of the over-excitation limiter (OEL) were formulated explicitly to capture the dynamic behaviour of the system. In [12], a sensitivity approach based on linearized power flow equations was presented using MPC (or RHC) to control transmission voltages. Reference [13] also used the sensitivity based approach and a variable reference trajectory to adaptively determine the amount of load shedding for voltage control.

All the aforementioned methods are of the centralized architecture in which the control actions are implemented by a central controller. However, due to large scale interconnections among transmission networks spanning over a wide geographic regions, the centralized formulation of the RHC strategy may have some difficulties because of the huge computational cost and communication facility, requirement of the global knowledge of the system and a single point of failure. Moreover, with the introduction of deregulation and market liberalization in the power utilities, many of them are reluctant to disclose their local information. These facts have led to the distributed approach of RHC technique by many researchers [14 - 15]. A non-cooperative distributed RHC with neighbour-to-neighbour communication has been put forward in [14] to co-ordinate the LTC actions to prevent voltage collapse. The approach is based on the Nash equilibrium of different coordination areas; however this will not provide a globally optimal solution. A Lagrangian decomposition based optimal control scheme has been proposed in [15] in an iterative fashion to find the global optimal solution. The key idea behind this approach is to solve a local problem which is a sub-problem of the original global problem and update some parameters by a central controller until a convergence is achieved. This approach still needs a central controller to co-ordinate the sub problems to find the optimal solution. In [16-18], evolutionary algorithms are used to determine or improve voltage collapse margin for system planning purposes; however these are not generally suitable for dynamic type of optimisation in the receding horizon control, as system conditions and operating points change continuously during an emergency.

This paper proposes a novel emergency voltage and reactive power control approach based on the multi-agent structure of RHC scheme using optimality condition decomposition (OCD) to decompose the overall problem into several sub-problems, each to be solved by an individual agent. An on-line distributed optimization technique is employed based on the linearized steady state model of the system. The optimization problem is formulated as a quadratic programming problem and an algorithm for global co-ordination is presented to get the optimum operating point. The agents only require communication with the neighbours, and no central co-ordinator is necessary for the convergence of the algorithm.

2.0 Multi-agent Receding Horizon Control

Receding Horizon Control (RHC) is one of the most widely used advanced control strategies which has been successfully applied in the process industries [19]. One of the most useful features of this framework is the ability to handle input and output constraints efficiently by formulating a discrete-time control model of the system. The conceptual structure of the RHC approach is shown in Fig. 1. The main idea is to formulate an on-line optimization problem subject to input and output constraints which results in a sequence of future control actions over a control horizon (N_C) given a system model in hand. The output is predicted over a prediction horizon (N_P) which is usually different from N_C. The first sequence of the so-computed actions is actually implemented and the process is repeated at the next sampling time when new measurements are available.

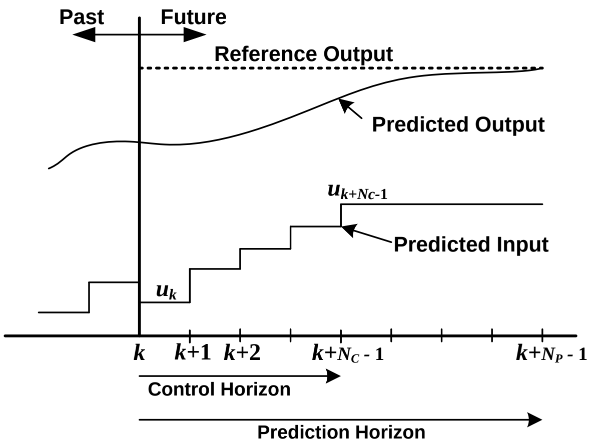

Fig. 1. Conceptual diagram of RHC

According to Fig. 1, a set of admissible control sequence **u**= $\{u_k, u_{k+1},\ldots.. u_{k+Nc-1}\}$ is computed at a given discrete time instance k to minimize the output trajectory deviation from the desired reference set point over the prediction horizon with minimum control efforts. In the single agent architecture, this optimization is performed by a central controller. The central agent thus requires the knowledge of the complete model of the system and the system-wide measurement should be available to the agent.

In a multi-agent receding horizon control (MARHC), multiple control agents use RHC where each agent is assigned to control a sub-system which is a part of overall system [20]. The agents first evaluate the sub-system states, compute the best control actions for the predicted sub-system state and input evolution and then implement actions. The actions that an agent takes in a MARHC structure influence both the evolution of its own sub-system and the evolution of the sub-system connected to it. Since the agents usually have no global overview and can access only a limited portion of the overall network, the future sub-system state prediction becomes uncertain without any interactions among the agents. Therefore, a communication network must be established among the agents (see Fig. 2). The challenge in implementing such a multi-agent RHC strategy is thus to ensure that the combined actions selected by all the agents should approach a similar result obtained from the actions selected by a single agent which has a complete knowledge of the system.

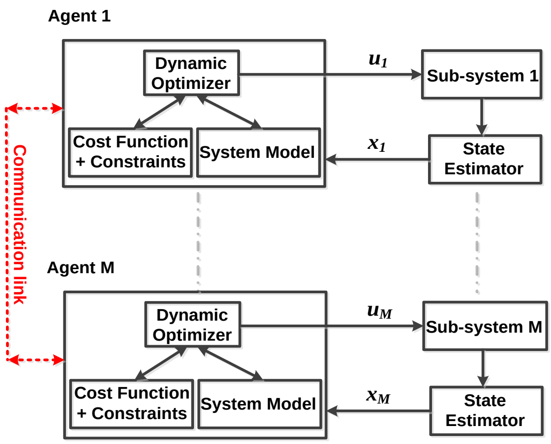

Fig. 2. Multi-agent receding horizon control

3.0 System modelling

Provided that the short term dynamics are stable, the dynamics of the RHC-based voltage control are predominantly associated with the long-term dynamics. In this context, one can resort to the Quasi-Steady State (QSS) model of the system in which the short term dynamics of the system are replaced by their equilibrium conditions. The QSS model for long term equilibrium can be written in a compact form as shown in (1) [21, 22]:

$$\mathbf{f}\left(\mathbf{x},\mathbf{u}\right)=\mathbf{0} \tag{1}$$

where u is the vector of control variables (generator voltages and real and reactive power loads) and x is the vector of the algebraic state variables. Eqn. (1) can be linearized at a known operating point to obtain the incremental relationship between the control and state variables which can be presented as:

$$\mathbf{f_x}d\mathbf{x}+\mathbf{f_u}d\mathbf{u}=\mathbf{0} \tag{2}$$

where $\mathbf{f_x}$ and $\mathbf{f_u}$ are the Jacobian matrices of **f** with respect to **x** and **u**. If $\mathbf{f_x}$ is non-singular, one can obtain the change in the state variables due to the change in the control variables as:

$$d\mathbf{x}=-\mathbf{f_x}^{-1}\mathbf{f_u}d\mathbf{u} \tag{3}$$

Let φ(**x**,**u**) be a quantity of interest which is a function of both the state variables and the control variables. Therefore, the change in φ due to a change in **u** can be obtained as:

$$d\phi=\nabla_\mathbf{x}\phi d\mathbf{x}+\nabla_\mathbf{u}\phi d\mathbf{u}=-\nabla_\mathbf{x}\phi\mathbf{f_x}^{-1}\mathbf{f_u}d\mathbf{u}+\nabla_\mathbf{u}\phi d\mathbf{u}=\left(\nabla_\mathbf{u}\phi-\nabla_\mathbf{x}\phi\mathbf{f_x}^{-1}\mathbf{f_u}\right)d\mathbf{u} \tag{4}$$

where $\nabla_\mathbf{u}\phi$ and $\nabla_\mathbf{x}\phi$ are the gradients of φ with respect to **u** and **x**, respectively. Hence, the sensitivity of φ to **u** is given by:

$$\frac{\partial\phi}{\partial\mathbf{u}}=\nabla_\mathbf{u}\phi-\nabla_\mathbf{x}\phi\mathbf{f_x}^{-1}\mathbf{f_u} \tag{5}$$

Equation (5) can be used to obtain the sensitivity of load voltages and generator reactive powers to the control variables and a linear model of equation (1) can be derived.

3.1 The objective function in a Centralized scheme

The overall objective is to minimize the changes in the control variables over the control horizon while satisfying the voltage and generator reactive power limits based on the measurements received at a specific time instance *k*. From a centralized point of view, this can be expressed as a quadratic programming problem [23] and can be defined as:

$$\min\sum_{i=1}^{N_C}\left\|\Delta\mathbf{u}\left(k+i\right)\right\|_\mathbf{R}^2 \tag{6a}$$

subject to

$$\mathbf{u}^{\min}\le\mathbf{u}\left(k+i\right)\le\mathbf{u}^{\max} \tag{6b}$$

$$\Delta \mathbf{u}^{\min} \leq \Delta \mathbf{u}\left(k+i\right) \leq \Delta \mathbf{u}^{\max} \tag{6c}$$

$$\mathbf{V_L}\left(k+i\right) = \mathbf{V_L}\left(k+i-1\right) + \frac{\partial \mathbf{V_L}}{\partial \mathbf{u}} \Delta \mathbf{u}\left(k+i\right) \tag{6d}$$

$$\mathbf{Q_G}\left(k+i\right) = \mathbf{Q_G}\left(k+i-1\right) + \frac{\partial \mathbf{Q_G}}{\partial \mathbf{u}} \Delta \mathbf{u}\left(k+i\right) \tag{6e}$$

$$\mathbf{V_L^{\min}} \leq \mathbf{V_L}\left(k+i\right) \leq \mathbf{V_L^{\max}} \tag{6f}$$

$$\mathbf{Q_G^{\min}} \leq \mathbf{Q_G}\left(k+i\right) \leq \mathbf{Q_G^{\max}} \tag{6g}$$

for i=1,…..,N_c

The objective (6a) minimizes the future deviation of the control variables over the control horizon N_c. As far as the long-term voltage instability scenarios are concerned, there is no clear advantage to take the prediction horizon N_p different than N_c [10]. Hence, the prediction horizon is considered equal to the control horizon. **R** is a diagonal weight matrix that penalizes expensive control variables with higher weights. Equations (6b) and (6c) impose the limits on the control variables. Equation (6d) and (6e) are the sequence of load voltage vector $\mathbf{V_L}$ and the vector of generator reactive power $\mathbf{Q_G}$ over the control horizon N_c, respectively. $\frac{\partial \mathbf{V_L}}{\partial \mathbf{u}}$ and $\frac{\partial \mathbf{Q_G}}{\partial \mathbf{u}}$ are the sensitivity matrix of load voltages and generator reactive powers to the control variables, respectively. The constraints (6f) and (6g) aim at limiting the load voltages and generators reactive power within their admissible limits.

3.2 MARHC Problem Formulation

We consider a multi-area power system which has M sub-systems (i.e. areas), where each sub-system consists of a set of generators and loads. The interactions among the sub-systems are established by the tie lines. The nodes that are connected to the tie lines are denoted as the boundary nodes for each sub-system.

An agent is assigned for each sub-system in MARHC framework (see Fig. 2) to control reactive power and load voltages in its associated sub-system by manipulating the generator terminal voltages and applying load shedding. It is assumed that the agent does not have an access to the information of the other sub-systems. Therefore, it uses RHC to obtain the best control sequence in the control horizon based on the model of its own sub-system and tries to improve its solution via communication with the neighbouring sub-systems. The agents work in a co-operative manner [24], i.e. they help each other to improve the overall cost function.

Each agent is required to solve a RHC problem as conveyed by equation (6). However, the agent cannot independently solve the problem due to the following reasons:

1. The sensitivities of load voltages and generator reactive powers with respect to the control variables in each area will depend on the state variables of the whole system i.e. these sensitivities are global quantities.

2. Each agent will try to optimize its local decision variables. The control action in one sub-system may affect another sub-system's state due to the relative coupling between them. Therefore, the optimal decision for one agent may not be the optimal decision for the overall problem.

Due to the fact mentioned above, a decomposition scheme to decompose the overall problem into sub-problems is proposed in this paper which can be solved in a coordinated way to find the global optimal solution. This also complies with the proposed MARHC scheme that the task of the emergency voltage control problem is shared by multiple agents; each is in-charge of its associated sub-system.

4.0 Multi area system modelling

Fig. 3 illustrates the equivalent systems for a two area power system. The sub-systems/areas are connected by tie-lines. In the equivalent model, each area preserves the actual model of its sub-system and replaces the neighbouring sub-systems by the voltage and angle of the neighbouring boundary node(s). For the sake of simplicity, only one boundary node per area is shown but the concept can be extended without any loss of generality to any number of boundary nodes and any number of neighbouring areas.

The decomposed equivalent steady-state model of the above system can be expressed as:

$$\mathbf{f}_1\left(\mathbf{x}_1, \mathbf{u}_1, V'_{b2}, \theta'_{b2}\right) = 0 \tag{7a}$$

$$V'_{b2} = V_{b2} \tag{7b}$$

$$\theta'_{b2} = \theta_{b2} \tag{7c}$$

$$\mathbf{f}_2\left(\mathbf{x}_2, \mathbf{u}_2, V'_{b1}, \theta'_{b1}\right) = 0 \tag{8a}$$

$$V'_{b1} = V_{b1} \tag{8b}$$

$$\theta'_{b1} = \theta_{b1} \tag{8c}$$

Equation (7a) indicates the steady state model for sub-system 1. $\mathbf{x}_1$ refers to the state variables and $\mathbf{u}_1$ refers to the control variables of sub-system 1. Note that the boundary voltage V'_{b2} and angle θ'_{b2} are appended in equation (7a) because the power flow equations of the boundary buses of sub-system 1 depend on these variables. These two variables are constrained through equations (7b-7c) which are the coupling equations for the model of sub-system 1. These equations imply that the variables V'_{b2} and θ'_{b2} must be equal to the actual variables V_{b2} and θ_{b2} respectively. This ensures that for a given system state and input set, the same solution will be obtained using the model (7) and (8) as would have been obtained from the model (1) [15].

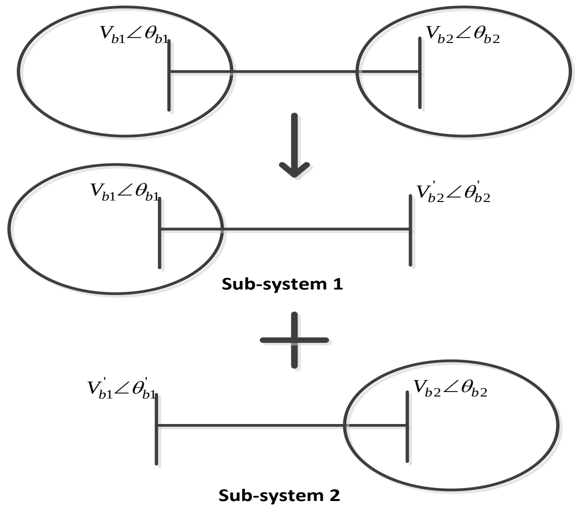

Fig.3. Decomposed model of a two area system

The equivalent MARHC problem of the problem in (6) for the decomposed model of (7)-(8) can be stated as:

$$\min \sum_{i=1}^{N_C} \left(\left\| \Delta \mathbf{u_1}(k+i) \right\|_{\mathbf{R_1}}^2 + \left\| \Delta \mathbf{u_2}(k+i) \right\|_{\mathbf{R_2}}^2 \right) \tag{9a}$$

subject to

$$\mathbf{u_1^{min}} \le \mathbf{u_1}(k+i) \le \mathbf{u_1^{max}} \tag{9b}$$

$$\mathbf{u_2^{min}} \le \mathbf{u_2}(k+i) \le \mathbf{u_2^{max}} \tag{9c}$$

$$\Delta\mathbf{u_1^{min}} \le \Delta\mathbf{u_1}(k+i) \le \Delta\mathbf{u_1^{max}} \tag{9d}$$

$$\Delta\mathbf{u_2^{min}} \le \Delta\mathbf{u_2}(k+i) \le \Delta\mathbf{u_2^{max}} \tag{9e}$$

$$\mathbf{V_{L1}}(k+i) = \mathbf{V_{L1}}(k+i-1) + \frac{\partial \mathbf{V_{L1}}}{\partial \mathbf{u_1}} \Delta\mathbf{u_1}(k+i) + \frac{\partial \mathbf{V_{L1}}}{\partial V_{b2}} \Delta V_{b2}(k+i) + \frac{\partial \mathbf{V_{L1}}}{\partial \theta_{b2}} \Delta\theta_{b2}(k+i) \tag{9f}$$

$$\mathbf{Q_{G1}}(k+i) = \mathbf{Q_{G1}}(k+i-1) + \frac{\partial \mathbf{Q_{G1}}}{\partial \mathbf{u_1}} \Delta\mathbf{u_1}(k+i) + \frac{\partial \mathbf{Q_{G1}}}{\partial V_{b2}} \Delta V_{b2}(k+i) + \frac{\partial \mathbf{Q_{G1}}}{\partial \theta_{b2}} \Delta\theta_{b2}(k+i) \tag{9g}$$

$$\mathbf{V_{L2}}(k+i) = \mathbf{V_{L2}}(k+i-1) + \frac{\partial \mathbf{V_{L2}}}{\partial \mathbf{u_2}} \Delta\mathbf{u_1}(k+i) + \frac{\partial \mathbf{V_{L2}}}{\partial V_{b1}} \Delta V_{b1}(k+i) + \frac{\partial \mathbf{V_{L2}}}{\partial \theta_{b1}} \Delta\theta_{b1}(k+i) \tag{9h}$$

$$\mathbf{Q_{G2}}(k+i) = \mathbf{Q_{G2}}(k+i-1) + \frac{\partial \mathbf{Q_{G2}}}{\partial \mathbf{u_2}} \Delta\mathbf{u_2}(k+i) + \frac{\partial \mathbf{Q_{G2}}}{\partial V_{b1}} \Delta V_{b1}(k+i) + \frac{\partial \mathbf{Q_{G2}}}{\partial \theta_{b1}} \Delta\theta_{b1}(k+i) \tag{9i}$$

$$\mathbf{V_{L1}^{min}} \le \mathbf{V_{L1}}(k+i) \le \mathbf{V_{L1}^{max}} \tag{9j}$$

$$\mathbf{Q}_{\mathbf{G1}}^{\min} \leq \mathbf{Q}_{\mathbf{G1}}\left(k+i\right) \leq \mathbf{Q}_{\mathbf{G1}}^{\max} \tag{9k}$$

$$\mathbf{V}_{\mathbf{L2}}^{\min} \leq \mathbf{V}_{\mathbf{L2}}\left(k+i\right) \leq \mathbf{V}_{\mathbf{L2}}^{\max} \tag{9l}$$

$$\mathbf{Q}_{\mathbf{G2}}^{\min} \leq \mathbf{Q}_{\mathbf{G2}}\left(k+i\right) \leq \mathbf{Q}_{\mathbf{G2}}^{\max} \tag{9m}$$

$$V_{b2}^{'}\left(k+i\right) = V_{b2}\left(k+i\right) \quad \theta_{b2}^{'}\left(k+i\right) = \theta_{b2}\left(k+i\right) \tag{9n}$$

$$V_{b1}^{'}\left(k+i\right) = V_{b1}\left(k+i\right) \quad \theta_{b1}^{'}\left(k+i\right) = \theta_{b1}\left(k+i\right) \tag{9o}$$

for $i = 1,\ldots..,N_c$

In (9a), the centralized objective function is split into two parts, where the first part belongs to sub-system 1 and the second part belongs to sub-system 2. All the variables in equation (9) relate to the variables in (6) while the sub-scripts 1 or 2 indicate that the variables belong to sub-system 1 or 2, respectively. The sensitivities in equation (9f-9g) and equation (9h-9i) are derived using the sensitivity formula (5) based on the linearized model of (7a) and (8a), respectively. Note that the boundary voltage and angle of the neighbouring sub-system are considered as inputs to the sub-system under consideration because they reflect the impact of the neighbouring sub-system. Thus, these variables are considered as decision variables in the optimization routine which are constrained through equation (9n-9o) to ensure that the solution stemming from optimization problem (9) is identical to the solution of the problem (6).

The constraints (9n-9o) are called complicating constraints because they involve variables from different sub-systems. The complicating constraints prevent the sub-systems to solve the optimization problem independently. Therefore, a mathematical decomposition technique is required to separate the problem (9) into a set of sub-problems so that each sub-problem can be solved independently by the associated agent.

Various decomposition techniques of the optimization problem having complicating constraints have been proposed in the literature; mostly using the Lagrangian and the augmented Lagrangian theory [25]. In a Lagrangian decomposition approach, the complicating constraints are relaxed and a Lagrange multiplier or dual variable is associated with each relaxed constraint. Then the sub-problems are solved independently with the relaxed constraints added to the objective function. A master co-ordinator is used to update the dual variables. The sub-problems are repeated with the updated dual variables until some convergence criteria are met [26]. A modified Lagrangian decomposition technique based on the decomposition of the first order optimality condition is proposed in [27]. This method has an excellent performance over the traditional Lagrangian decomposition approach and has been applied to many multi-area optimal power flow and state estimation problems in recent years [28], [29], [30] and [31].

4.1 Proposed Optimality Condition Decomposition

The optimality condition decomposition (OCD) is a modified Lagrangian decomposition approach in which the global optimization problem is decomposed into several sub-problems in such a way that if the first-order Karush-Kuhn-Tucker (KKT) optimality conditions of every sub-problem are joined together, they are identical to the first-order optimality conditions of the global problem [30]. The area sub-problem is obtained by relaxing all the complicating constraints of other areas through adding them to the objective function of the area sub-problem and maintaining its own complicating constraints. The sub-problem is then solved iteratively by fixing the optimization variables of other sub-systems that are known from previous iteration. Based on the aforementioned idea, the global MARHC problem (9) can be decomposed into area sub-problems as follows.

Sub-problem 1:

$$\min \sum_{i=1}^{N_c} \left(\left\| \Delta \mathbf{u_1} \left(k+i\right) \right\|_{\mathbf{R_1}}^2 + \overline{\lambda_{v1}\left(k+i\right)} \left(\overline{V_{b1}^{'}\left(k+i\right)} - V_{b1}\left(k+i\right) \right) + \overline{\lambda_{\theta 1}\left(k+i\right)} \left(\overline{\theta_{b1}^{'}\left(k+i\right)} - \theta_{b1}\left(k+i\right) \right) \right) \tag{10a}$$

subject to constraints (9b, 9d, 9f, 9g, 9j, 9k)

$$V_{b2}^{'}\left(k+i\right) = \overline{V_{b2}\left(k+i\right)} : \lambda_{v2}\left(k+i\right) \tag{10b}$$

$$\theta_{b2}^{'}\left(k+i\right) = \overline{\theta_{b2}\left(k+i\right)} : \lambda_{\theta 2}\left(k+i\right) \tag{10c}$$

for i=1……N_c

Sub-problem 2:

$$\min \sum_{i=1}^{N_c} \left(\left\| \Delta \mathbf{u_2} \left(k+i\right) \right\|_{\mathbf{R_2}}^2 + \overline{\lambda_{v2}\left(k+i\right)} \left(\overline{V_{b2}^{'}\left(k+i\right)} - V_{b2}\left(k+i\right) \right) + \overline{\lambda_{\theta 2}\left(k+i\right)} \left(\overline{\theta_{b2}^{'}\left(k+i\right)} - \theta_{b2}\left(k+i\right) \right) \right) \tag{11a}$$

subject to constraints (9c, 9e, 9h, 9i, 9l, 9m)

$$V_{b1}^{'}\left(k+i\right) = \overline{V_{b1}\left(k+i\right)} : \lambda_{v1}\left(k+i\right) \tag{11b}$$

$$\theta_{b1}^{'}\left(k+i\right) = \overline{\theta_{b1}\left(k+i\right)} : \lambda_{\theta 1}\left(k+i\right) \tag{11c}$$

for $i = 1……N_c$

The objective functions (10a) and (11a) now include the complicating constraints for the adjacent sub-system which are multiplied by the Lagrange multipliers associated with these constraints. The lines over the variables indicate the known value of the variables from previous iteration or trial values for the first iteration. Thus, each sub-problem aims to minimize the cost of its own sub-system together with the cost of the contribution from the neighbouring sub-systems as conveyed by the relaxed complicating constraints. In the above procedure, the Lagrange multipliers are updated by maintaining the sub-problem's own complicating constraints (constraints (10b) and (10c) for sub-problem 1 and constraints (11b) and (11c) for sub-problem 2).

4.2 Proposed Co-ordination Algorithm

The main advantage of the above described procedure for MARHC is that it does not require a central co-ordinator to update the Lagrange multiplier as in the case of common Lagrangian decomposition algorithm. Further, the convergence of the algorithm is relatively faster and the computational efficiency is improved (see [30] for the proof of the convergence). The control is initiated when an agent finds any violation of load voltage and/or generator reactive power in its sub-system, mostly after any contingency event. The only information that the agent needs to share with the neighbouring agents are the boundary voltages and angles and Lagrange multipliers associated with the complicating constraints. The step by step procedure for the proposed MARHC algorithm is described as follows (for sub-system 1):

1) At a given time instant *k*, collect measurement and derive the sensitivity based model of the sub-system.

2) Perform the optimization problem in (10) over a control horizon N_c. For this purpose,

a) Initialize the boundary variables $V'_{b1}(k+i)$, $\theta'_{b1}(k+i)$, $V_{b2}(k+i)$ and $\theta_{b2}(k+i)$ and the Lagrange multipliers $\lambda_{v2}(k+i)$ and $\lambda_{\theta 2}(k+i)$ for i=1,………, N_c. This is Iter = 0;

b) Solve (10a) subject to the constraints (10b) and (10c).

c) Transmit the updated values of the boundary variables $V_{b1}(k+i)$, $\theta_{b1}(k+i)$, $V'_{b2}(k+i)$ and $\theta'_{b2}(k+i)$ and Lagrange multipliers $\lambda_{v1}(k+i)$ and $\lambda_{\theta 1}(k+i)$ for k = 1,………, N_c to sub-system 2.

d) Receive the updated values of the boundary variables $V'_{b1}(k+i)$, $\theta'_{b1}(k+i)$, $V_{b2}(k+i)$ and $\theta_{b2}(k+i)$ and the Lagrange multipliers $\lambda_{v2}(k+i)$ and $\lambda_{\theta 2}(k+i)$ for i = 1,………, N_c from sub-system 2.

e) If they don't change significantly, stop, go to step (3) else Iter = Iter + 1. Repeat step (b) to (d).

3) Apply the first sequence of the so computed actions to the practical system.

4) $k = k + 1$, repeat step 1 to 3 until all the load voltages and reactive power outputs are within the admissible limits.

The above algorithm is carried out in sub-system 2 in the similar manner and therefore, is not described here. Note that the algorithm is not initiated by all the agents at the same time; rather it is initiated by the agent that has found any constraint violation in its sub-system. The other agents will participate in the algorithm by receiving the boundary variables and Lagrange multipliers from the neighbouring agent. In this way, the proposed procedure will traverse from one sub-system to another sub-system.

4.3 Issues for Real time implementation of the proposed MARHC

The proposed MARHC algorithm can be implemented to find the optimal solution of the global problem in a distributed way without disclosing the internal information of the sub-systems. However, this comes with a price of an iterative process among the agents which will increase with the number of boundary variables and Lagrange multipliers. To apply the proposed algorithm for real time voltage control in a receding horizon concept, several issues should be taken under consideration:

1) As has been stated earlier, the long term voltage collapse scenario is typically monotonic lasting from tens of seconds to several minutes. This indicates that the RHC scheme can be implemented with longer sampling time and shorter control horizon. This will allow relatively longer amount of time for the agents in the MARHC scheme to perform the iterative algorithm as well as reduction in the number of iterations to converge because of the reduced number of boundary variables.

2) It can be observed that the sensitivities are updated from one time instant to another. However, the sensitivity matrices do not vary significantly because of the "linear" nature of the voltage decay problem and thus can be computed only at the beginning of the prediction horizon which will reduce the computation time. This assumption can be compensated for by the feedback nature of the algorithm at the next sampling instant when the sensitivities will be updated with new collected measurements.

3) Depending on the communication facility of the system, a maximum limit can be imposed on the iteration number of the algorithm or the solution can be obtained with a certain degree of accuracy. Moreover, it should be noted that the agents communicate only with the neighbours. As the voltage instability is typically a local phenomenon and local countermeasures are the most effective, the algorithm can be restricted within a limited region of the system where disturbance occurs.

4.4 Tuning of constraints in the control horizon

The advantage of the receding horizon strategy lies in the ability to gradually correct the voltages and generator reactive powers along the control horizon instead of doing that in a single step. This can be implemented by enforcing the limits on the constraints (9j) to (9m) only at the end of the control horizon [11]. But this may lead to slow voltage recovery and generator reactive power correction. Moreover, some voltages and reactive powers which were within the limits before the control action starts may violate the limits in the intermediate steps which is not desirable. Therefore, a time varying limit on the voltage and reactive power constraint along the control horizon has been considered in this paper. If the voltage or reactive power is out of the admissible limit at the start of the control horizon, that limit varies linearly along the control horizon. This means that the limit is not considered as a hard limit along the control horizon. Rather it gradually becomes satisfied at the end of the horizon which is the inherent benefit of the receding horizon control. For example, if a load voltage is 0.9 pu at the beginning of the horizon and the control horizon consists of 2 time steps, then at first time step the limit will be 0.925 pu and at the second time step the limit would be 0.95 pu which is the admissible steady state limit of the load voltage. Equations 12(a) – 13(c) show the steady-state minimum and maximum limits of the load voltages and reactive powers in the generator buses.

$$V_L^{min}(k+i) = V_L(k) + \frac{\mathrm{V_L^{min}} - V_L(k)}{N_c - i + 1} \quad \text{if } V_L(k) < \mathrm{V_L^{min}} \tag{12a}$$

$$V_L^{max}(k+i) = V_L(k) + \frac{\mathrm{V_L^{max}} - V_L(k)}{N_c - i + 1} \quad \text{if } V_L(k) > \mathrm{V_L^{max}} \tag{12b}$$

$$V_L^{min}(k+i) = \mathrm{V_L^{min}} \qquad V_L^{max}(k+i) = \mathrm{V_L^{max}} \qquad \text{otherwise} \tag{12c}$$

$$Q_G^{min}(k+i) = Q_G(k) + \frac{\mathrm{Q_G^{min}} - Q_G(k)}{N_c - i + 1} \quad \text{if } Q_G(k) < \mathrm{Q_G^{min}} \tag{13a}$$

$$Q_G^{max}(k+i) = Q_G(k) + \frac{\mathrm{Q_G^{max}} - Q_G(k)}{N_c - i + 1} \quad \text{if } Q_G(k) > \mathrm{Q_G^{max}} \tag{13b}$$

$$Q_G^{min}(k+i) = \mathrm{Q_G^{min}} \qquad Q_G^{max}(k+i) = \mathrm{Q_G^{max}} \qquad \text{otherwise} \tag{13c}$$

for $i = 1 \ldots\ldots N_c$

where $\mathrm{V_L^{min}}$ ($\mathrm{V_L^{max}}$) is the steady-state minimum (maximum) limit of the load voltage and $\mathrm{Q_G^{min}}$ ($\mathrm{Q_G^{max}}$) the reactive power limit of the synchronous generator. The generator reactive power limit should be compatible with the reactive capability curve. Hence, the reactive power limit is calculated based on the received snapshot of terminal voltage and real power generation (see [21], equations (3.32a), (3.32b) and (3.49)), where the effect of saturation is neglected for the sake of simplicity.

4.5 Generator voltage set-point and reactive power

As the terminal voltage of the generator is considered as a control variable, it should be noted that this control is implemented by changing the AVR reference voltage which is usually different from the actual terminal voltage. Based on the fact that a change in AVR reference voltage results in almost equal change in the terminal voltage [11], the controller changes the AVR reference voltage by the amount equal to the desired terminal voltage correction.

The generator reactive power under over excitation (OXL) control of the excitation system (i.e. constant field current) is given by

$$Q_g = \frac{VI_{FD}^{\max}}{X_d}\cos\left(\delta-\theta\right) - V^2\left(\frac{\sin^2\left(\delta-\theta\right)}{X_q} + \frac{\cos^2\left(\delta-\theta\right)}{X_d}\right) \tag{14}$$

This clearly shows that the reactive power is dependant on the generator terminal voltage. As the OXL tends to lower the AVR reference voltage to control the excitation current, the terminal voltage of the generator also gradually falls. As a result, the reactive power also gradually falls under OXL control.

Generator bus voltage is used as control variable due to the fact that the generator excitation control is able to control the voltage directly and can adjust the bus voltage. Load shedding is another control variable that is used in the proposed method, when the countermeasures are not sufficient. In the proposed method, the on-load tap changers (LTC) are also allowed to vary automatically within the time frame before load shedding is activated.

5.0 Validation of the proposed method using Case Studies

The proposed MARHC is implemented on Nordic-32 test system [32, 33] shown in Fig. 4. The system consists of 52 buses, 20 synchronous machines and 22 loads. This system composes of four areas: “North” with hydro generation and some load, “Central” with much load and thermal power generation, “Equiv” connected to the “North” which includes a very simple equivalent of an external system, and “South” with thermal generation, rather loosely connected to the rest of the system. The system has rather long transmission lines of 400-kV nominal voltage. Five lines are equipped with series compensation. The model also includes a representation of some regional systems operating at 220 and 130 kV, respectively [33]. Simulations have been carried out using PSAT and MATLAB.

To capture the realistic scenario of long term voltage instability, a detailed dynamic model of the generators with automatic voltage regulator (AVR) and over-excitation limiter (OEL) is considered. The OEL was modelled to follow either inverse time or fixed time characteristics. All the loads are supplied through distribution transformers having automatic load tap changer (LTC). A delay of 30 seconds is considered for the first tap movement. The subsequent tap changes have shorter delays but vary from each other ranging from 9 to 12 seconds to prevent the unrealistic tap synchronization. An exponential model for the load is used with exponent 1 (constant current) for active power and exponent 2 (constant impedance) for reactive power.

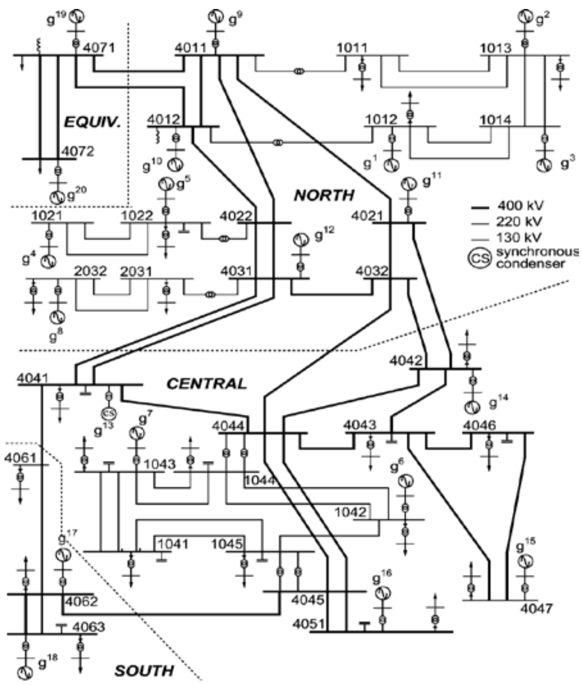

Fig. 4. Single-line diagram of Nordic32 test system.

As shown in Fig. 4, the system is composed of four areas, namely North, Central, Equivalent, and South. North area is generation reach-area with hydro generation and some loads and Central area is load-reach area with thermal power generation. For the purpose of illustration of the proposed MARHC, each of these areas was considered as a sub-system and was assigned an agent to solve the optimization sub-problem as given in (10).

Each agent is able to change the generator voltages in the range of 0.95-1.1 p.u. and curtails a maximum of 30 percent of the load at each bus in its area. The associated weights for the controls in the optimization are 1 for generator voltages and 100 for load shedding. The proposed MARHC was implemented with a sampling time of 20 seconds and control horizon of 40 seconds.

Case 1: Single contingency: Outage of line 4032-4044

This case involves the outage of a tie line 4032-4044 between North and Central area without any fault, after 5 seconds of the start of the simulation. The evolution of three transmission voltages without the proposed MARHC is shown in Fig. 5. The system settles to a short-term equilibrium after the electromechanical oscillations have died out. The LTCs start acting at 35 seconds. Subsequently, the voltages evolve under the effect of LTCs trying to restore distribution voltages and OELs limiting the field currents of the generators. The voltage instability of the power system eventually leads to voltage collapse in less than three minutes after the initiating the disturbance.

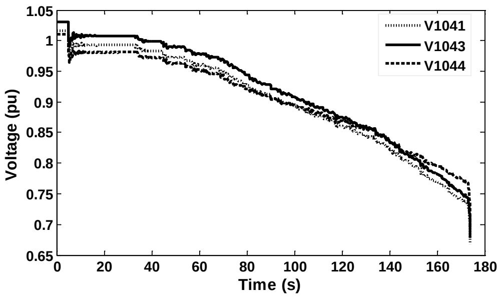

Fig. 5. Transmission voltages without MARHC

Fig. 6 shows the evolution of the field currents for some of the field limited generators in the central area. After settling to the post disturbance values, they start increasing from t = 35s, when the OLTCs start acting. The actions of OEL subsequently limit the field currents of generator 14 (Gen 14), generator 15 (Gen 15) and generator 16 (Gen 16), causing the generators to produce constant field current and hence constant reactive power rather leading to the release of constant voltage constraint.

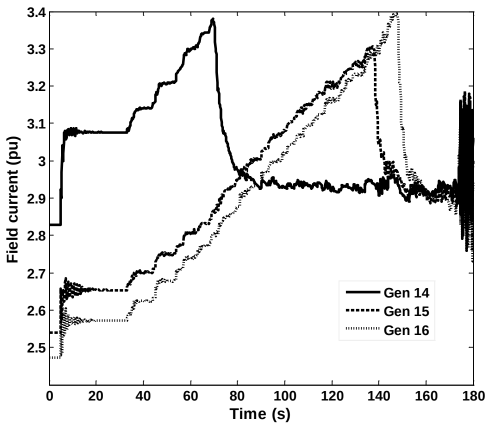

Fig. 6. Field currents of limited generators in central area without MARHC

The control action is initiated by the agents in Central area as it detects the maximum reactive power violation in generator 14. It is assumed that the agents wait for a short period to take into account the line auto-reclosure time and to allow the transients to die out to find the steady-state measurement. In this case, the first control action is implemented at 30 seconds followed by consecutive actions at a 20 seconds interval. The termination condition for the algorithm is set by a tolerance of .0001 for the boundary variables and Lagrange multipliers. The evolution of the transmission voltages stabilized by the proposed MARHC is shown in Fig. 7.

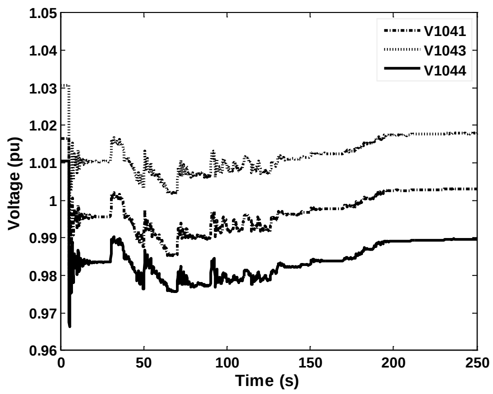

Fig. 7. Transmission voltages in case 1 with proposed MARHC

Fig. 8 shows the change in AVR reference voltages in some generators as requested by the proposed MARHC. No load shedding occurs in this case because the generator voltage set-point adjustment is sufficient to eventually stabilize the voltages. The system is stabilized before 230 seconds and no control actions are further issued after this time.

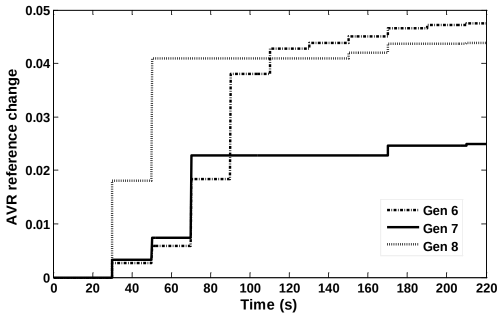

Fig. 8. Change in AVR reference voltage by the proposed MARHC in case 1

Using the convergence criteria as described earlier, the algorithm converges between 26 to 34 iterations at each sampling instant. Simulation was carried out with a tolerance of 0.001 and the number of iterations required is from 16 to 20. The number of iterations is quite small compared to the Lagrangian decomposition approach as shown in [20]. Moreover, the agents do not need to communicate with a central controller; they only need to communicate with their immediate neighbours which will reduce the time for communication in the proposed MARHC algorithm. Fig. 11 shows the evolution of some of the Lagrange multipliers at the first sampling step.

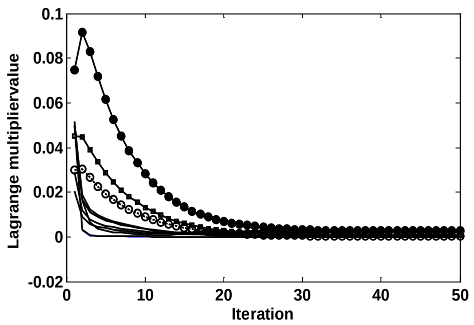

Fig. 9. Evolution of the Lagrange multiplier in case 1

Case 2: Multiple Contingency- Outage of parallel lines 4044-4045

This case represents a double line outage scenario. The contingency involves the outage of one of the parallel lines between bus 4044 and 4045 at 5 seconds after the simulation starts. At 20 seconds, the other line between bus 4044 and 4045 also goes out of service. Fig. 10 shows the voltage evolution in this case without any countermeasures. The voltages decay more rapidly in this case than in case 1 and undergo long-term instability by collapsing at 153 seconds.

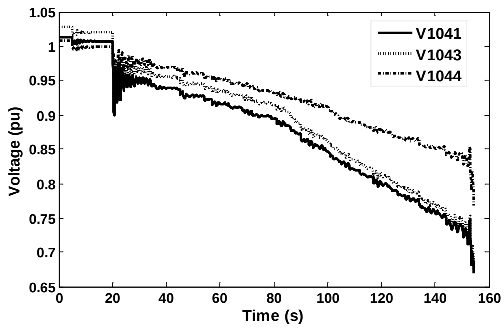

Fig. 10. Evolution of transmission voltages in case 2

Fig. 11 shows the voltage evolution under the operation of the proposed MARHC. The control action is initiated by the central area agent and the first control is applied at 30 seconds. The MARHC manipulates the generator voltages at first few steps (see Fig. 12) to control the voltages and reactive powers. Due to the severity of the contingency, this countermeasure is not sufficient to stabilize the system. Therefore, load shedding occurs at t = 70 seconds (to shed 21.386 MW) and at t = 110 seconds (to shed 8.9 MW further).

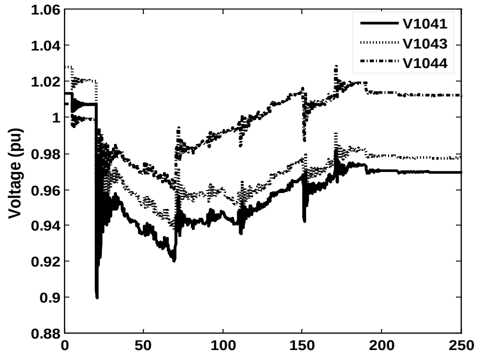

Fig. 11. Voltage stabilization by proposed MARHC in case 2

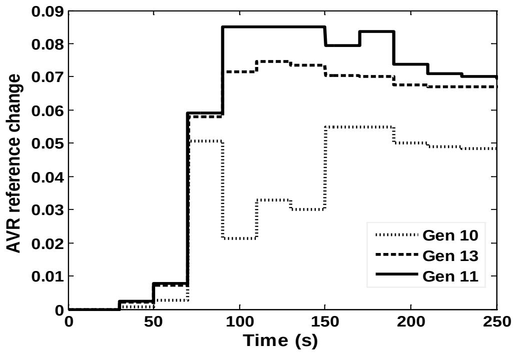

Fig. 12. Change in AVR reference voltage by the proposed MARHC in case 2

Case 3: Load increase scenario

This case demonstrates a load increase scenario together with a single line outage between bus 4041 and 4061 which is tie line between Central and South area. The loads in the Central area are linearly increased from 20 seconds to 120 seconds by a total amount of 100 MW. The voltage collapse occurs at t = 213.3 seconds in this case (see Fig. 13).

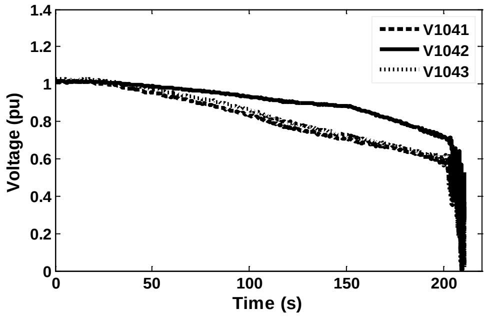

Fig. 13. Evolution of transmission voltages in case 3

Fig. 14 shows the system response with the MARHC controller in action. The proposed MARHC smoothly stabilizes the system mainly with the control of the generator terminal voltages (see Fig. 15) and the system settles to a post-disturbance equilibrium at t = 250 seconds. A very little amount of load shedding (5.6 MW) occurred at t = 210 seconds.

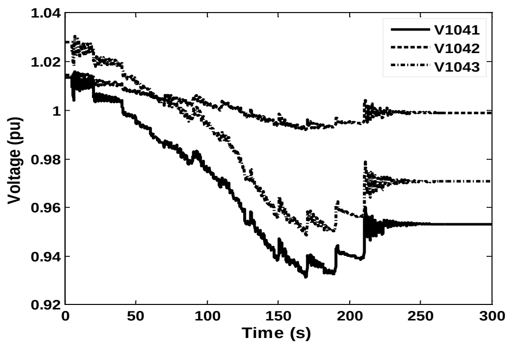

Fig. 14. Voltage stabilization by proposed MARHC in case 3

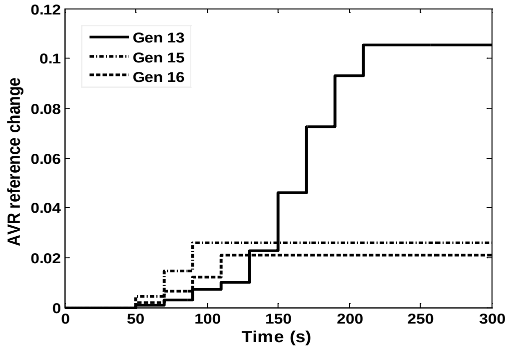

Fig. 15. Change in AVR reference voltage by the proposed MARHC in case 3

The optimization routine directly gives the amount of load (active and reactive power) that needs to be shed. A constant power factor is preserved from the original load in the load shedding algorithm, such that if 10MW is shed at any bus, a proportional amount of reactive power is also shed to ensure that the power factor remains constant. This practice is also adopted in [11,12]. We also follow the practice described in [11], where a load less than 0.1 MW is assumed to be so small that no shedding will be carried out on this type of load.Table 1 shows the final optimal values of generator voltages after the system is stabilized in per unit. Table 2 shows the bus number and the amount of load shedding in MW. A constant power factor has been preserved for the load shedding as adopted in [11,12].

Table 1: The optimal values of the generator bus voltage in per unit

Bus Number	Case 1	Case 2	Case 3
1	1.1000	1.0975	1.0960
2	1.0375	1.0416	1.0709
3	1.0610	1.0931	1.0720
4	1.1000	1.0564	1.0548
5	1.0876	1.0844	1.0505
6	1.0421	0.9838	1.0174
7	1.0306	0.9530	1.0008
8	1.0855	1.0732	1.0646
9	1.0682	1.0602	1.0517
10	1.0625	1.0558	1.0448
11	1.0484	1.0832	1.0241
12	1.0326	1.0484	1.0110
13	1.0904	1.1000	1.0490
14	1.0158	1.0654	1.0195
15	1.0766	1.0951	1.0572
16	1.0940	1.0960	1.0714

17	1.0356	1.0947	1.0331
18	0.9879	1.0697	1.0565
19	1.0807	1.0338	1.0556
20	1.0414	0.9545	1.0319

Table 2: The optimal values of load shedding in MW in the subsystems under control – CENTRAL and SOUTH areas(The Power factor of the original load is preserved)

Bus Number	Case 1 No load shed	Case 2	Case 3
1041	0	9.989	0.7
1042	0	0.919	0.33
1043	0	4.652	0.59
1044	0	0.84	0.49
1045	0	6.552	0.5
4041	0	0	0.18
4042	0	0	0.29
4043	0	0.202	0.47
4046	0	0.136	0.61
4047	0	0	0.33
4051	0	5.384	0.4
4061	0	0.561	0.26
4062	0	0.646	0.25
4063	0	0.405	0.21

Case 4: Testing the Effectiveness of the Proposed Approach

To demonstrate the effectiveness of the proposed approach, a comparative study is carried out in this section. The proposed approach is compared with a traditional approach. Also computational time is estimated to indicate the suitability for real-time application of the proposed method.

Comparison with Traditional Lagrangian Relaxation Approach:

In this case study, the performance of the proposed MARHC is compared with the traditional Lagrangian relaxation (LR) approach. All of the above described scenarios have been tested using the LR approach. A sub-gradient method has been used to update the Lagrange multipliers associated with the complicating constraints [34]. As can be seen from Table 3, the maximum number of iterations to converge to the optimal solution is greater for the LR approach compared to the OCD approach used in the proposed MARHC.

Table 3. Maximum number of iterations in OCD and LR

	Maximum no. of iteration	
	OCD	LR
Case 1	34	178
Case 2	39	201
Case 3	28	144

v

Fig. 16 shows the evolution of the Lagrange multiplier in both the approach. The value of the Lagrange multiplier in proposed MARHC approach converges quickly within 34 iterations while an oscillatory behaviour can be observed for the LR approach. The LR approach took 178 iterations to converge to the desired tolerance.

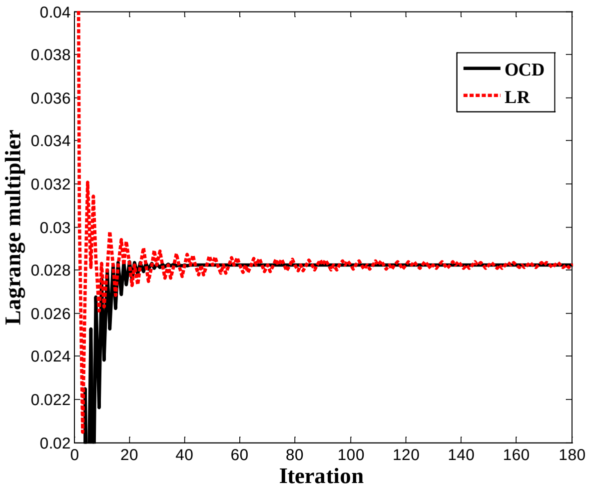

Fig. 16. Evolution of the Lagrange multiplier

Computational time and communication delay:

The total number of iterations required to converge to an optimal solution by the proposed MARHC for the cases 1 to 3 was in the range of 19 to 38. The algorithm was implemented in MATLAB running in a Windows XP machine with Core(TM) i7 CPU and 3.55 GB of RAM. The computation time considered in this paper is the time to solve the optimization sub-problem based on the information received at each sampling instance. The total number of iterations required to converge to an optimal solution for each sub-problem for cases 1 to 3 was in the range of 19 to 38. The maximum time taken by an iteration was 9.7 msec and therefore the maximum time taken to solve each sub-problem for the convergence would be 368.6 msec. With regards to the communication speed among the agents, it will depend upon the bandwidth of the communication channel and the delay in collecting data through local measurements. With the advent of synchronized phasor measurement techniques in power systems [35], the data through local measurements can be collected in real-time. As the proposed MARHC is based on only neighbour to neighbour communication, the communication delay among the agents will also be less. As indicated in [36], the wide-area network based on high speed optical fibre network with 155.52 Mbps can facilitate to communicate over 180 km distance with a delay time of 1.3 msec. Assuming that the radius of each area or sub-system does not surpass more than 100 km, a total maximum delay of 548.8 msec may incur in the cases described above. Thus, in a worst-case scenario, an overall delay of 917.49 msec may occur that includes computational time as well as communication delay.

6.0 Conclusions

A multi-agent based receding horizon control to prevent voltage collapse during an emergency is illustrated in this paper. The proposed control scheme is developed based on the optimality condition decomposition of the global optimization problem with neighbour-to-neighbour communication among the agents. A distributed control in a multi-agent environment is used as a cooperative framework in which each agent can preserve its local information and communicate with neighbouring agents to mutually agree and provide a best solution. Various scenarios were created to validate the robustness of the proposed method and results presented. The main advantages of the proposed method are that no central controller is required to make a decision and the convergence of the proposed method is faster compared to the traditional Lagrangian decomposition method. The overall computation and communication requirement are relatively small and within the reach of the modern communication facility of a power system.

7.0 Acknowledgement

This work is supported by the Australian Research Council (ARC) and Transgrid Linkage Grant, LP0991428. The authors gratefully acknowledge the financial support and cooperation from TransGrid.

References:

[1] "Final report on the August 14, 2003 blackout in the United States and Canada: Causes and recommendations," US-Canada Power System Outage Task Force, 2004, accessed in Nov 2013. [Online]. Available: http://energy.gov/sites/prod/files/oeprod/DocumentsandMedia/BlackoutFinal-Web.pdf

[2] "Final report: System disturbance on 4 November, 2006," Union for the Co-ordination of Transmission of Electricity (UCTE), 2007, accessed in Nov 2013. [Online]. Available: www.geocities.jp/ps_dictionary/blackout/Final-Report-20070130.pdf

[3] P. Kundur and et al, "Definition and classification of power system stability IEEE/CIGRE joint task force on stability terms and definitions", *IEEE Trans. on Power Systems*, vol. 19, No. 3, pp. 1387-1401, 2004.

[4] S. K. Chang, F. Albuyeh, M. Gilles, G. Marks, and K. Kato, "Optimal real-time voltage control," *IEEE Trans. Power Syst.*, vol. 5, no. 3, pp. 750 – 758, Aug. 1990.

[5] D. Popovic, V. Levi, and Z. Gorecan, "Co-ordination of emergency secondary-voltage control and load shedding to prevent voltage instability," *IEE Proceedings-Generation, Transmission and Distribution*, vol. 144, no. 3, pp. 293 – 300, 1997.

[6] H. Vu, P. Pruvot, C. Launay, and Y. Harmand, "An improved voltage control on large-scale power system," *IEEE Trans. Power Syst.*, vol. 11, no. 3, pp. 1295 – 303, 1996.

[7] B. Marinescu and H. Bourles, "Robust predictive control for the flexible coordinated secondary voltage control of large-scale power systems," *IEEE Trans. Power Syst*., vol. 14, no. 4, pp. 1262 – 8, 1999.

[8] M. Larsson, D. J. Hill, and G. Olsson, "Emergency voltage control using search and predictive control," *Int. J. Elect. Power Energy Syst.*, vol. 24, pp. 121–130, 2002

[9] J. Wen, Q. Wu, D. Turner, S. Cheng, and J. Fitch, "Optimal coordinated voltage control for power system voltage stability," *IEEE Trans. Power Syst*., vol. 19, no. 2, pp. 1115 – 22, 2004.

[10] L. Jin, R. Kumar, and N. Elia, "Model predictive control-based real-time power system protection schemes," *IEEE Trans. Power Syst*., vol. 25, no. 2, pp. 988 – 998, 2010.

[11] M. Glavic, M. Hajian, W. Rosehart, and T. Van Cutsem, "Receding horizon multi-step optimization to correct nonviable or unstable transmission voltages," *IEEE Trans. Power Systems*, vol. 26, no. 3, pp. 1641–1650, Aug. 2011.

[12] Mahdi Hajian, William Rosehart, Mevludin Glavic, Hamidreza Zareipour, Thierry Van Cutsem, "Linearized Power Flow Equations Based Predictive Control of Transmission Voltages," *46th Hawaii International Conference on System Sciences (HICSS)*, 2013, 7-10 Jan. 2013, pp. 2298-2304, 2013.

[13] T. Amraee, A. M. Ranjbar and R. Feuillet, "Adaptive under-voltage load shedding scheme using model predictive control", *Electric Power Systems Research*, Volume 81, Issue 7, July 2011, Pages 1507-1513.

[14] M. Moradzadeh, R. Boel, L. Vandevelde, "Voltage Coordination in Multi-Area Power Systems via Distributed Model Predictive Control," *IEEE Transactions on Power Systems*, vol.28, no.1, pp.513,521, Feb. 2013

[15] A. Beccuti, T. Demiray, G. Andersson, and M. Morari, "A Lagrangian decomposition algorithm for optimal emergency voltage control," *IEEE Trans. Power Syst*., vol. 25, no. 4, pp. 1769–1779, Nov. 2010.

[16] S. H. Goh, T. P. Saha, Z. Y. Dong, "Solving Multi-Objective Voltage Stability Constrained Power Transfer Capability Problem using Evolutionary Computation", *International Journal of Emerging Electric Power Systems*, Vol. 12, Issue 1, pp. 5.1-5.22, 2011.

[17] D. Šošić, , I. Škokljev, "Evolutionary algorithm for calculating available transfer capability", *Journal of Electrical Engineering*, Volume 64, Issue 5, Pages 291-297, 2013.

[18] Y. Liu, L. Zhang, Y. Zhao, "Calculation of static voltage stability margin based on continuous power flow and improved differential evolution algorithm", *International Journal of Digital Content Technology and its Applications,* Vol. 6, No. 17, Pages 86-95, September 2012.

[19] E. F. Camacho and C. Bordons, " Model Predictive Control" *London: Springer Verlag*, 2004.

[20] R.R. Negenborn, "Multi-agent model predictive control with applications to power networks", PhD Thesis, University of Delft, 2007

[21] T. Van Cutsem and C. Vournas, *Voltage Stability of Electric Power Systems*. Boston, MA: Kluwer, 1998.

[22] M. Glavic and T. Van Cutsem, "Some reflections on model predictive control of transmission voltages," *38th North American Power Symp. (NAPS)*, Carbondale, IL, Sep. 2006.

[23] G. Valverde, T. Van Cutsem, "Model Predictive Control of Voltages in Active Distribution Networks," *IEEE Transactions on Smart Grid*, vol.PP, no.99, pp.1-10, 2013.

[24] J.M. Maestre, D. Munoz de la Pena, E.F. Camacho, "Distributed model predictive control based on a cooperative game", *Optimal Control Applications and Methods* Volume 32, Issue 2, pp. 153-176, March/April 2011

[25] A. J. Conejo, R. Minguez, E. Castillo, and R. Garcia-Bertrand, *Decomposition Techniques in Mathematical Programming*. New York: Springer, 2006.

[26] D. Bertsekas, *Nonlinear Programming*. Nashua, NH: Athena Scientific,1995.

[27] A. J. Conejo, F. J. Nogales, and F. J. Prieto, "A decomposition procedure based on approximate Newton directions," *Math. Program.*, pp.495–515, 2002.

[28] F. J. Nogales, F. J. Prieto, and A. J. Conejo, "A decomposition methodology applied to the multi-area optimal power flow problem," *Ann.Oper. Res.*, no. 120, pp. 99–116, 2003.

[29] M. Granada, Marcos J. Rider, J.R.S. Mantovani and M. Shahidehpour, "A decentralized approach for optimal reactive power dispatch using Lagrangian decomposition method", *Electric Power System Research*, Volume 89, pp-148-156, August 2012.

[30] A. J. Conejo, S. de la Torre, and M. Canas, "An optimization approach to multiarea state estimation," *IEEE Tranactions Power Syst.*, vol. 22, no. 1,pp. 213–221, Feb. 2007.

[31] F. Milano, "An open source power system analysis toolbox," *IEEE Tranactions on Power Systems*, vol. 20, no. 3, pp. 1199–1206, Aug. 2005.

[32] M. Stubbe, "Long-term dynamics phase II, *Report of CIGRE Task Force* 32.02.08 1995.

[33] T. V. Cutsem, "Description, Modeling and Simulation Results of a Test System for Voltage Stability Analysis Version 4. January 2013, University of Li`ege, Belgium.

[34] Bertsekas, D. *Constrained Optimization and Lagrange Multiplier Methods*. Academic Press, New York, 1982.

[35] A. G. Phadke and J. S. Thorp, *Synchronized Phasor Measurements and Their Applications*. New York: Springer, 2008.

[36] X. Tong, X. Wang, R. Wang, F. Huang, X. Dong, K.M. Hopkinson, G. Song, "The Study of a Regional Decentralized Peer-to-Peer Negotiation-Based Wide-Area Backup Protection Multi-Agent System," *IEEE Transactions on Smart Grid*, , vol.4, no.2, pp.1197,1206, June 2013